PLASMA–SURFACE RELATED THREE-DIMENSIONAL MODELING RESULTS FOR WENDELSTEIN 7-X AND EAST

F. SCHLUCK
Forschungszentrum Jülich GmbH
Jülich, Germany
Email: f.schluck@fz-juelich.de

M. RACK
Forschungszentrum Jülich GmbH
Jülich, Germany

S. XU
Forschungszentrum Jülich GmbH and University of Science and Technology
Jülich, Germany and Hefei, China

W. ZHOLOBENKO
Max-Planck-Institut für Plasmaphysik
Garching, Germany

J. COSFELD
Forschungszentrum Jülich GmbH
Jülich, Germany

D. REITER
Forschungszentrum Jülich GmbH
Jülich, Germany

Y. FENG
Max-Planck-Institut für Plasmaphysik
Greifswald, Germany

Abstract

Present-day fusion devices are operated with a multitude of diagnostics in different locations, with which important insight in plasma properties is obtained. However, since the detected signals only represent a spatially small part of the machine, the experiment natively exhibits blind spots, in particular in the three dimensional edge plasma region, where flux surface averaging reductions are inappropriate. Theory, and especially numerical simulation, may bridge over these unknown areas in order to complete the complex physical picture of the nature of plasma properties.

The fluid plasma edge Monte-Carlo code EMC3 coupled to the kinetic (neutral) transport code EIRENE is a commonly used fully dimensional plasma edge simulation code for treating such complex magnetic configurations. EMC3 bases on a Monte-Carlo algorithm for a reduced set of Braginskii equations formulated in a Fokker-Planck scheme, while EIRENE solves extended Boltzmann equations in full phase-space directly.

Because of its intrinsically 3D structure, one of the main applications of EMC3-EIRENE is the simulation of scrape-off layer physics for the stellarator Wendelstein 7-X. However, also in tokamaks 3D effects may play an important role, e.g. when using resonant magnetic perturbations to control the formation of edge localized modes.

The paper presents recent results obtained with EMC3-EIRENE related to plasma–surface interaction. This computational tool is applied to intrinsically 3D Lower-Hybrid Wave induced magnetic perturbation modeling on the Experimental Advanced Superconducting Tokamak (EAST). The divertor manipulator concept and design, effective charge state distribution modeling and the helium beam synthetic diagnostic concept are major applications for Wendelstein 7-X.

Certain minority ions might not reach thermodynamic equilibrium before meeting a loss channel, which renders a fluid description invalid. Key additions in the kinetic description of such charged particles in EIRENE are introduced and investigated at the example of helium plasma limiter operation in Wendelstein 7-X.

1. INTRODUCTION

Theoretical physics in the magnetic confinement fusion plasma boundary aspires both, to deepen the understanding of often complex plasma–surface-related problems and proposing directions of future scientific ambitions. While analytic models might provide a comprehensive picture of sub-aspects in the underlying processes, they often fail to capture the extensive physics in such electromagnetics-hydrodynamics-materials interplays. It is numerical simulation which potentially expands the theoretical toolkits by an additional access-channel. Modeling of the plasma edge region, where flux surface averaging reductions are either infeasible or inappropriate, has become an important activity in fusion research.

The fluid plasma edge code (EMC3) [1] coupled to the kinetic (neutral) transport code EIRENE [2, 3] is a commonly used fully three-dimensional plasma edge simulation Monte-Carlo code for treating such complex magnetic configurations. EMC3 bases on a Monte-Carlo algorithm for a reduced set of (Braginskii) diffusion-advection equations formulated in a Fokker-Planck scheme [4, Ch. 4.1], while EIRENE solves an extended Boltzmann equation directly in the full 6D phase-space, for minority species and ballistic transport effects.
Because of its intrinsically 3D structure, one of the main applications of EMC3-EIRENE is the simulation of scrape-off layer physics for the stellarator Wendelstein 7-X. However, also in tokamak physics 3D effects may play an important role, e.g. when using resonant magnetic perturbations in order to control the formation of edge localized modes [5] or other symmetry breaking effects.

Actively optimizing edge magnetic topology on tokamaks by feasible mechanisms is an attractive topic for future fusion reactors [6]. Recent experiments from EAST show that LHWs can produce magnetic perturbations by inducing helical current filaments flowing along magnetic field lines in the scrape-off layer. The code package EMC3-EIRENE is used to model the influence of LHW-induced magnetic perturbations on edge plasma transport, as the results [7] show very good qualitative agreement between simulation and experiment.

In addition to our tokamak research, we focus mainly on Wendelstein 7-X, where probe manipulators are used as one of the most important diagnostics to gain insight in the plasma−wall interaction processes. These interactions typically include material erosion, deposition, or impurity migration pathways. Currently, a manipulator directly mounted in the divertor region is in development and planned to be ready with the high-heat-flux divertor. With EMC3-EIRENE simulations we obtain heat fluxes and plasma profiles, which subsequently are used to perform more reduced simulations to study the power loads on the plasma facing components. This is a fundamental study to evaluate both the physical and technological requirements in the divertor manipulator concept [8].

A further aspect is the development of an iterative approach to post-dict the spatially distributed effective charge state and (effective) mass in impure hydrogen plasmas in Wendelstein 7-X [9]. Experimentally, this quantity could not be measured during the first plasma operation phase and it is only measured very locally in the second plasma operation phase. However, the effective charge state is a key parameter to evaluate e.g. Langmuir probe measurements.

EIRENE is used intensively for simulating a synthetic diagnostic that resembles the experimental helium beam measurements on Wendelstein 7-X [10]. With this, physical processes behind temperature and density measurements are analyzed in more detail. In the same context an update of atomic data for helium has been performed within EIRENE.

The combined code package EMC3-EIRENE is in constant development. It has been extended in order to handle minority ions or impurities in a hybrid approach, i.e. in a fluid-kinetic manner. In the very first operation phases, Wendelstein 7-X was often operated with helium plasmas, which will most likely also be the case for ITER. The hybrid treatment is a substantial adjustment in order to properly describe ions at low collisionality, while keeping the overall computational effort as slim as possible [11].
So far, the kinetic ion treatment in EIRENE incorporated only a simple energy relaxation model. By now it has received an importantly extending modification, featuring e.g. drift motion [12], mirror force and cross-field diffusion accounting for turbulence. With this development version of EIRENE, previous analysis of Wendelstein 7-X with EMC3-EIRENE will be revisited, treating He^+ in kinetic description for relevant 3D edge plasma configurations. Conclusions on different density distributions are drawn to emphasize the significance of the implemented features.

2. MAGNETIC PERTURBATIONS INDUCED BY LOWER-HYBRID WAVES

Recent experiments from the Experimental Advanced Superconducting Tokamak (EAST) show that lower hybrid waves (LHWs) can profoundly change the magnetic topology by inducing helical current filaments flowing along magnetic field lines in the scrape-off layer [13, 14, 15]. With EMC3-EIRENE simulations we investigate how these magnetic perturbations caused by LHWs affect the edge plasma transport [7].

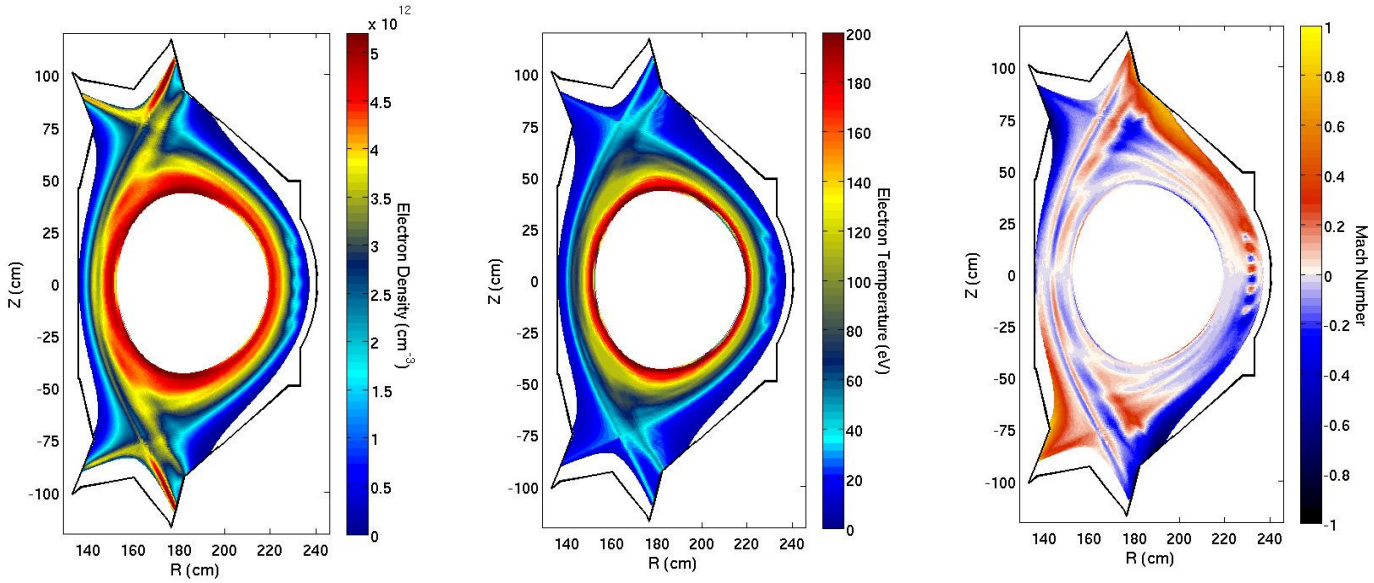

FIG. 1. The poloidal cross-sections of the electron density, electron temperature and Mach number simulated by the EMC3-EIRENE code at the same toroidal position with the LHW antenna for a perturbed (by RMPs) plasma.

Fig. 1 shows the cut-through of the three-dimensional distribution of electron density, electron temperature, as well as the Mach number of plasma flow along the magnetic field at the same toroidal position with the LHW antenna. The 3D magnetic topology structure induced by LHWs is reflected obviously in these plasma properties, because of much stronger parallel field transport compared to the cross-field diffusion. The plasma boundary formed with lobe structures near the X-points at the low field side, which can be regarded as the additional plasma transport channel, reaches out towards the divertor target, thus resulting in the strike line splitting. The additional plasma transport channel caused by LHWs can not only increase the radial transport of the edge plasma, but also significantly cause the redistribution of heat load between inner and outer divertor targets. For the Mach number, there is a poloidal oscillation of the parallel flow direction inside the separatrix, and the pattern of parallel flow with alternating direction is aligned to the radial position of the main resonances and related to their respective poloidal mode number.

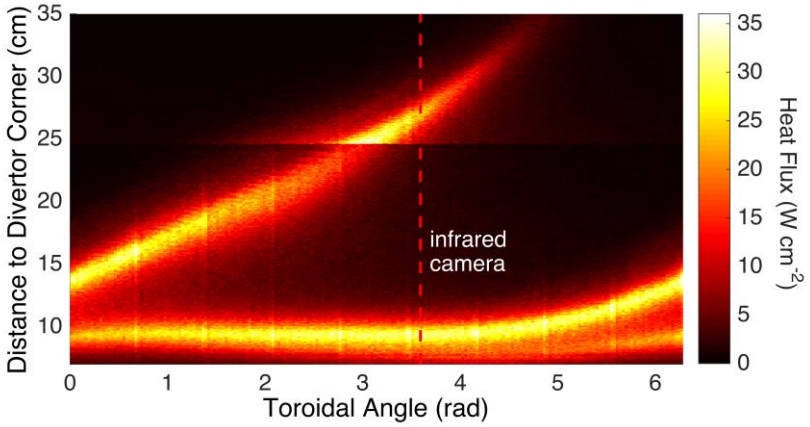

FIG. 2. Simulated heat flux footprint on the lower outer divertor targets.

To better understand the strike line splitting induced by helical magnetic lobes, Fig. 2 illustrates the heat flux footprint on the lower outer divertor. In this fixed view, it looks like one striation was split from the original strike line. In fact this behavior occurs due to the spiraling heat flux pattern, which is given by the dominant toroidal mode number of LHW-induced perturbation fields $n = 1$.

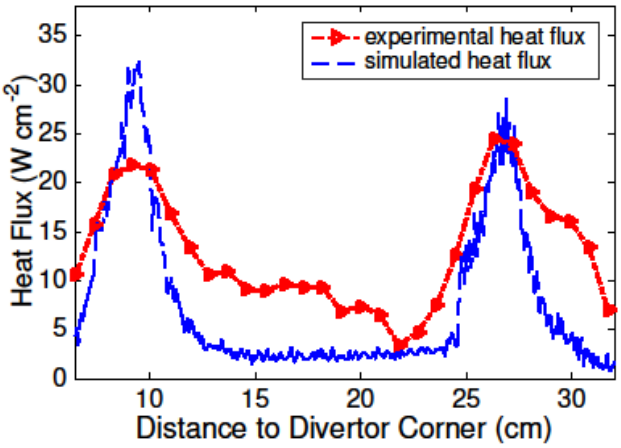

FIG. 3. Experimental (red) and simulated (dashed blue) heat flux on the lower outer divertor. The position of the infrared camera is indicated by the vertical dashed orange line in Fig. 2.

The simulated heat flux shows qualitative agreement with the experimental data measured by an infrared camera as shown in Fig. 3. Due to larger input power of LHWs in past experiments, one obtains deeper penetration and an extended stochastic layer. With EMC3-EIRENE simulations we show the consequence on the ratio of heat flux between the split striated and the original strike line on the divertor targets.

3. DIVERTOR MANIPULATOR CONCEPT STUDIES

One direct application of EMC3-EIRENE contributing to engineering questions is the development of a divertor manipulator for Wendelstein 7-X [8]. Probe manipulators are a versatile addition to typical plasma edge diagnostics. Equipped with material samples they allow for detailed investigation of plasma−wall interaction processes, such as material erosion, deposition, or impurity transport pathways. Combined with electrical probes a study of scrape-off layer and plasma edge density, temperature, and flow profiles, as well as magnetic topologies is possible.

A mid-plane manipulator is already in operation on Wendelstein 7-X and its development was supported by field line tracing techniques to identify the best location for integrated measurement together with other down-stream diagnostics as well as EMC3-EIRENE predictions of plasma edge parameters. For the divertor manipulator we needed to study the critical issues of heat and power loads, power redistribution, and experimental access to the complex magnetic topology of Wendelstein 7-X.

Focus was put on the topological region that is accessible for the different coil current configurations and the power load on the manipulator with respect to the resulting different magnetic configurations. The qualitative analysis of power loads on plasma facing components is performed using a numerical tracer-particle diffusion tool [16]. EMC3-EIRENE simulations provided the required reference point in heat flux and plasma profiles for this simple model and therefore an essential input to perform the study on the divertor manipulator concept.

4. EFFECTIVE CHARGE STATE MODELING

Recently, we developed an iterative approach to post-dict the spatially distributed effective charge state Z_{eff} and effective mass m_{eff} in a Wendelstein 7-X hydrogen plasma with carbon impurities [9]. Experimentally, these quantities could not be measured during the first plasma operation phase and they are only measured very locally in the second plasma operation phase.

The procedure required many fine-tuned simulations followed by reinterpretation of diagnostic data that require the effective charge state and the effective mass as an input parameters. The simulations within the iterative process were constrained by measurements of the radiated power and up- and down-stream density/temperature profiles. Matching refined measurements in each iterative step via the free simulation parameters of EMC3 (mainly: anomalous radial transport coefficients) enabled a precise identification and quantification of the effective charge state and effective mass. Under the investigated experimental conditions, Z_{eff} and m_{eff} typically differ between the up- and down-stream probe positions by roughly 30% which has been ignored so fare in the experimental post-processing, see Fig. 4.

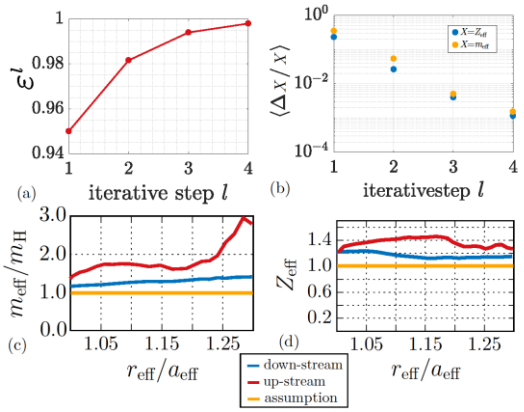

FIG. 4. Iterative process adjusting the separatrix density to find a converged effective mass and charge state. Radial profile of Z_{eff} and m_{eff} at the down- and up-stream location, showing significant deviations outside the last closed flux surface. The upper plots show the convergence behavior of the abovementioned iterative scheme.

5. SYNTHETIC HELIUM BEAM DIAGNOSTICS

Helium beam emission spectroscopy (BES) is an attractive technique for spatially resolved density and temperature measurements, applied at various tokamaks [17] and stellarators [18]. Robust approximations must be applied when extending the model to keep the complexity manageable. The EIRENE synthetic diagnostic has been often applied to analyze the emission of atomic and molecular hydrogen [19, 20]. Recently, the helium database was updated [21] and the diagnostic was extended for arbitrary atomic species [10], which now allows for reliably studying helium emission, particularly in BES applications.

The thermal spread of the He beam into the island divertor region of Wendelstein 7-X is simulated in 3D on an EMC3-EIRENE computed hydrogen plasma background [11]. We take into account elastic p-He scattering, meta-stable state transport and singlet-triplet state mixing due to the magnetic field, quantifying the impact of each effect. Synthetic camera pictures, as in Fig. 5, are then constructed by line-of-sight (LOS) integration of 3D emissivity profiles.

We find that for medium sized fusion experiments with B = 0.2 – 3.7 T, the magnetic field does not need to be taken into account explicitly. For higher magnetic fields, however, the effect of singlet-triplet state mixing is much more pronounced. Since differing collisional-radiative models are in use, we study the effect of a varying number of energy eigenstates, which strongly influences the measured temperature, in our model by a factor of up to 4.

The elastic p-He scattering does not directly influence the He emission. However, it alters the propagation into the plasma: especially at higher plasma densities, the beam is significantly widened and back-scattered. The helium cloud becomes more spherical than elongated, which in turn makes LOS integration effects much more severe, especially for the direct application of the common line ratio technique, since the emissivity profiles of different spectral lines are correlated. For an electron density of $3 \cdot 10^{13}$ cm^{-3} and an electron temperature of 10 – 60 eV, the effect on the temperature dependent line ratio of 728.1 nm and 706.5 nm lines is up to 40%.

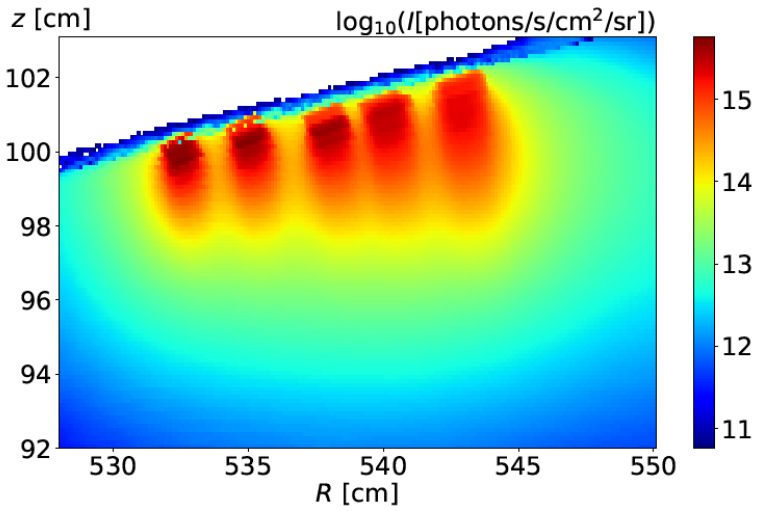

FIG. 5. A synthetic diagnostic measurement at arbitrary camera location for the Helium 667.8 nm line intensity from five simulated He beams in the vicinity of an upper Wendelstein 7-X island divertor.

6. ENHANCED KINETIC ION TRANSPORT

Minority ions in the plasma boundary might not thermalize in their lifespan which renders a kinetic treatment of these non-Maxwellian particles necessary [22]. EIRENE possesses a simple ion transport model containing energy relaxation and more physical effects were tested on two-dimensional tokamak geometries in other EIRENE-incorporating code packages [23]. Recently, we reported the technical implementation of drift effects in EIRENE for EMC3-EIRENE geometries [12].

We present results on helium plasma in Wendelstein 7-X in limiter configuration with enhanced kinetic ion transport features, namely newly implemented gradient B and curvature drifts, magnetic mirror force, and cross-field diffusion accounting for anomalous transport. For the numerical implementation, see the according poster. We chose a diffusion coefficient of $D = 1$ cm^2 / s in all following simulations. It has been shown [11] that He^+ has to be treated kinetically, which is why the kinetic ion features are expected to be of importance. Plasma case simulation specifications can be found in [11].

Fig. 6 shows a single He^+ trajectory starting at the brown / black star. We compare the classic EIRENE test ion transport (in brown and white in inset, respectively) to the enhanced description including drifts, mirror-force and cross-field transport. In the former this particle impacting the limiter (in purple) gets reflected and follows almost the same trajectory it came from. Once regarding the mirror force, the same particle deviates from its original orbit and turns the direction of flow. In the inset, which is slightly rotated, it can be seen that the limiter is hit a second time (teal stars mark the impact positions) and the test ion, consecutively, does turn once more. This way it conserves its sign of velocity with respect to its pre-impact flow. Although this is a single particle example it does illustrate the importance of incorporating the multitude of newly implemented physics for kinetic ions.

Regarding the newly implemented effects does influence more than just single particle trajectories. Consideration of cross-field diffusion, drifts, and the mirror force results for instance in varying density profiles which can be seen in Figs. 7 and 8.
The former shows the poloidal cross-section in the limiter region. We show atomic (left) and minority ionic densities (right) in cases of classic ion treatment in EIRENE. The central plot shows the absolute density difference between the classic and the enhanced cases, which is on the order of 10%. While for the He^+ density there is no obvious trend, we find that the different behaviour results in a reduced atomic density at the limiter. When only considering drifts and mirror force, the atomic density at the limiter does actually increase. In the case where only diffusion and mirror force are enabled, one finds a decrease of the atomic density at the limiter. Combining these findings with the density profile presented in Fig. 7 stresses that diffusion is the dominant effect in this helium limiter case on Wendelstein 7-X in the limiter location.

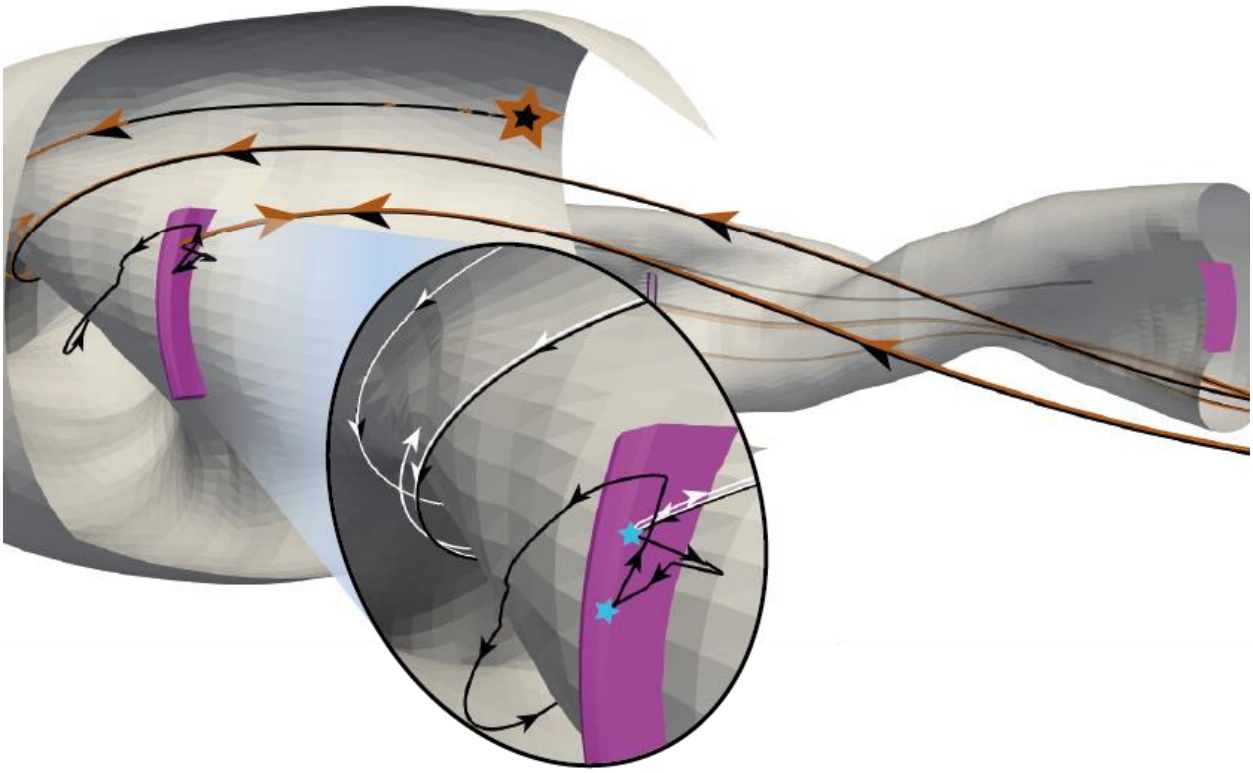

FIG. 6. Single He^+ trajectory for classic EIRENE ion transport (brown, white in inset) compared to enhanced transport (black) with the starting location indicated by the star. In the latter case, the test ion reflected at the limiter (in purple) turns due to the mirror force and follows its pre-impact direction. In classic ion transport, the test ion reflect off the limiter into almost the same trajectory it came from (arrows highlight the direction of flow).

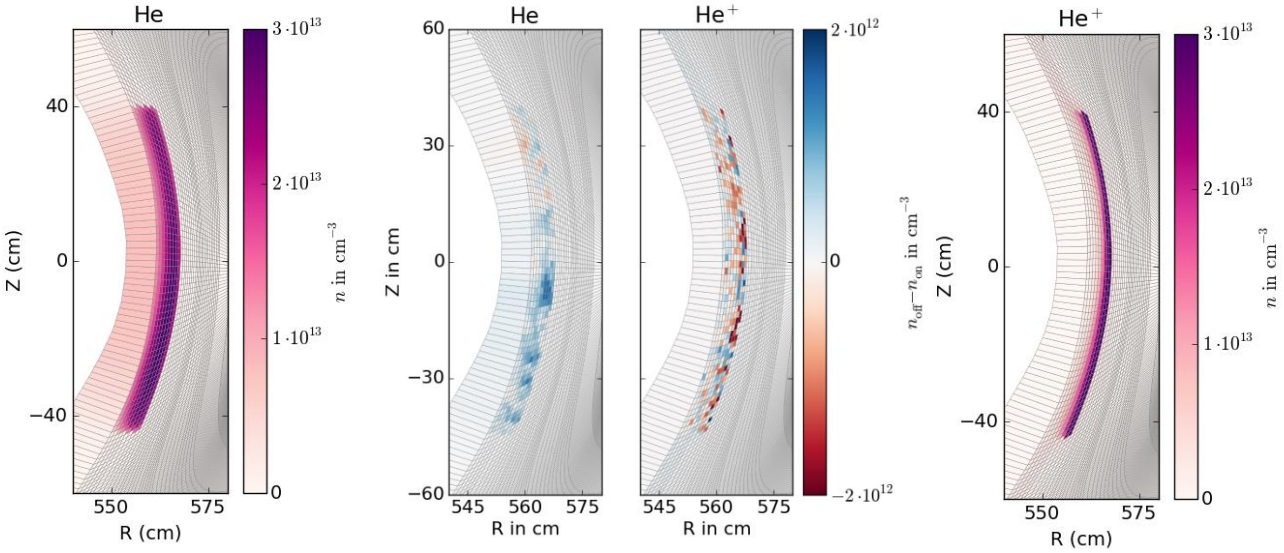

FIG. 7. Poloidal profiles of atomic (left) and minority ion density (right) obtained by classic kinetic ion treatment. Center: absolute difference (up to 10%) between atomic and ionic densities at the limiter (fixed toroidal angle).

In Fig. 8 one finds the three radial density profiles for He, He^+, and He^{2+} averaged over poloidal and toroidal direction, where the orange vertical line marks the last closed flux surface, separating the region of closed field lines (right) to open field lines (left of it). While one expects the density peak of He^+ to diminish, one finds overall a lower He^+ density, which is due to the fact that now this species can reach areas formerly inaccessible with the classic EIRENE ion transport. If reaching such areas, new loss channels, e.g. for ionization and neutralization, are opened.

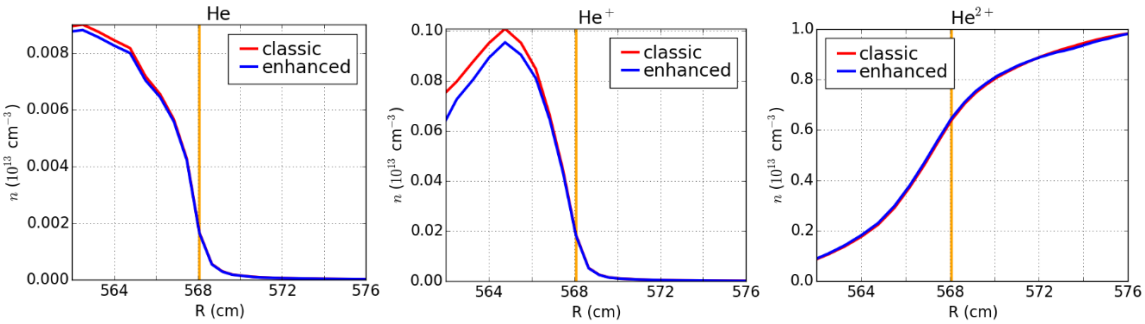

FIG. 8. Toroidally and poloidally averaged radial profiles of the different helium densities, obtained using classic and enhanced transport in EIRENE for He^+.

ACKNOWLEDGEMENTS

This work has been carried out within the framework of the EUROfusion consortium and has received funding from the Euratom research and training programme 2014-2018 under grant agreement No 633053. The views and opinions expressed herein do not necessarily reflect those of the European Commission.
The Authors gratefully acknowledge the computing time granted by the JARA-HPC Vergabegremium and VSR Comission on the supercomputer JURECA at Forschungszentrum Jülich.

REFERENCES

[1] FENG, Y. et al., Journal of Nuclear Materials, 266-269, 812 (1999)
[2] EIRENE. http://www.eirene.de on 27th Sep 2018
[3] REITER, D. et al., Fusion Science and Technology, 47 (2), 172 (2005)
[4] RISKEN, H., The Fokker-Planck Equation: Methods Of Solution And Applications, Springer, 2nd edition (1989)
[5] WAGNER, F. et al., Proceedings of 13th Conf. Plasma Phys. Cont. Fusion (IAEA, Vienna), vol. I, 277-90 (1982)
[6] LIANG, Y. et al., Physical Review Letters 98, 26, 265004 (2007)
[7] XU, S. et al., Nuclear Fusion 58, 106008 (2018)
[8] RACK, M. et al., Plasma Science and Technology, 20, 5, SI (2018)
[9] COSFELD, J. et al., Report JUEL-4414 (2018)
[10] ZHOLOBENKO, W. et al., Nuclear Fusion, accepted (2018)
[11] RACK, M. et al., Nuclear Fusion 57, 056011 (2017)
[12] SCHLUCK, F. et al., Conference Proceeding on EPS Plasma Physics (2018)
[13] LI, J. et al., Nature Physics 9, 817-21 (2013)
[14] LIANG, Y. et al., Physical Review Letters 110, 235002 (2013)
[15] RACK, M. et al., Nuclear Fusion 54, 064016 (2014)
[16] BOZHENKOV, S. et al., Fusion Engineering and Design, 88, 11, 2997 (2013)
[17] GRIENER, M. et al., Plasma Physics and Controlled Fusion, 60 (2), 025008 (2018)
[18] BARBUI, T. et al., Review of Scientific Instruments, 87 (11), 11E554 (2016)
[19] REITER, D. et al., Journal of Nuclear Materials 196-98, 1059 (1992)
[20] FRERICHS, H. et al., Nuclear Fusion 57 (12), 126022 (2017)
[21] GOTO, M., Journal of Quantitative Spectroscopy and Radiative Transfer 76 (3-4), 331 (2003)
[22] REISER, D. et al., Nuclear Fusion 2, 165-77, 38 (1998)
[23] SEEBACHER, J. et al., Computer Physics Communication 183, 947-59 (2012)